Cement & Concrete Composites 45 (2014) 89–101

Contents lists available at ScienceDirect

Cement & Concrete Composites

journal homepage: www.elsevier.com/locate/cemconcomp

Resistance of blended cement pastes subjected to organic acids: Quantification of anhydrous and hydrated phases

O. Oueslati, J. Duchesne *

Centre de Recherche sur les Infrastructures en Béton, Université Laval, 1065 Ave de la Médecine, Québec, QC G1V 0A6, Canada

ARTICLE INFO

Article history:
Received 1 August 2012
Received in revised form 12 July 2013
Accepted 13 September 2013
Available online 21 September 2013

Keywords:
Quantification
Anhydrous phases
Hydrates
Organic acids
NMR
Selective dissolution
Image analysis
Thermogravimetry
Granulated blast furnace slag
Metakaolin

ABSTRACT

Concrete for agricultural construction is often subject to aggressive environmental conditions. Ground granulated blast furnace slag (GGBFS) or metakaolin (MK) largely improve the chemical resistance of the binder. Anhydrous particles seem particularly resistant to the acid solution. The purpose of this study is to quantify anhydrous particles in blended cement pastes as a function of acid exposition time in order to evaluate their acid resistance.

Cement pastes were moist cured for 28 days and then immersed in an acetic acid solution for 2 months. The quantification of the anhydrous phases was carried out using ^{29}Si MAS NMR, selective dissolution and back-scattered electron (BSE) images analysis, while the hydrated phases content was evaluated by TGA. After 28 days of hydration, 60% of OPC, 44% of GGBFS and 76% of MK particles were hydrated. The amount of anhydrous particles drops for all materials during acid immersion. After 2 months of immersion, the amount of anhydrous particles drops by 49%, 23% and 15% for OPC, GGBFS, and MK respectively. This study confirms that GGBFS and MK anhydrous and hydrates phases present higher acid resistance than OPC.

1. Introduction

Agricultural effluents contain organic acids that constitute a severe chemical threat toward the concrete of agricultural structures. Acidic environments are among the most aggressive media for concrete. Cement hydration products are stable only in solutions with well defined Ca^{2+} and OH^- concentrations and in contact with an acidic environment, the constituents of the hardened cement pastes are altered by decalcification [1]. Organic acids react with hydrated and anhydrous compounds of the cement paste to give mainly calcium salts. Depending on their solubility, these salts may precipitate or may be dissolved in solution. Acids such as nitric, hydrochloric or acetic acids form easily soluble Ca-salts and have a strong decalcifying effect [2–5]. Bertron et al. [5] showed that the four acids of the liquid manure (acetic, propionic, butyric and iso-butyric acids) have an equivalent aggressiveness while lactic acid presents a greater aggressiveness according to its dissociation constant value (p*K*a). Moreover, it was demonstrated that an acetic acid solution of pH 4 mimics well the aggressiveness of organic acids found in animal manure. Due to the formation of easily soluble Ca-salts, acetic acid forms a porous altered layer with relatively weak diffusion resistance [1].

Previous studies [6–9] has shown that cement pastes blended with ground granulated blast furnace slag (GGBFS) and metakaolin (MK) largely improve the chemical resistance of the binder when submitted to an acidic environment. Chemical composition profiles measured by electron probe microanalyser (EPMA) of paste samples immersed in acetic acid solution according to the distance to the surface of the specimen have demonstrated the good chemical resistance of GGBFS and MK samples. These samples presented a reduced altered depth that is less decalcified compared to other binders [6]. Anhydrous GGBFS particles seemed particularly resistant against the acid attack and their presence can partly explain the good performance of that binder. The positive effect of residual anhydrous grains was also reported by Bertron et al. [10]. These authors reported that the amount of some anhydrous grains (slag grains, silica fume agglomerates and C_4AF) may improve the durability because they are not dissolved in the altered zone and their presence can help preserving the integrity of the matrix. These authors observed that the C_4AF grains were well preserved when subjected to an acetic acid solution at pH 4, while C_2S and C_3S grains were mainly dissolved.

According to Macias et al. [11], the acidic attack decomposes the unhydrated and hydrated cement paste phases. Portlandite is dissolved and the hydrated silicate and aluminate phases are decom-

* Corresponding author. Tel.: +1 418 656 2177.
E-mail addresses: olfa.oueslati.1@ulaval.ca (O. Oueslati), josee.duchesne@ggl.ulaval.ca (J. Duchesne).

0958-9465/$ - see front matter © 2013 Elsevier Ltd. All rights reserved.
http://dx.doi.org/10.1016/j.cemconcomp.2013.09.007

posed. The resistance of cement pastes is due to the nature of the hydration products rather than the porosity of the hardened cementing materials and depend on the protective silica layer precipitated on the surface [12]. As stated by Beddoe and Dorner [13], the dissolution of ferrite or aluminate hydrates is slower and occurs at lower pH values than the release of Ca^{2+} from C–S–H and portlandite. They indicated that as the pH decreases, portlandite (12.6), ettringite (10.7), C–S–H (≈10.5) and finally calcium aluminate and ferrite hydrates decompose successively.

All these studies have shown the beneficial effect of some SCMs on the durability of concrete submitted to acidic environments. However, although observations have shown large amounts of anhydrous grains presented in the degraded zone of samples submitted to organic acids, no study has focused on the quantification of anhydrous grains. The quantitative assessment of the rate of hydration of SCMs is still a challenge in the scientific community. Much effort is made to improve the methods. Some methods have been tested for slag cements, others for metakaolin. In this work, we evaluated different techniques recently developed to directly quantify the cement and SCMs anhydrous phases during the acid immersion.

The purpose of this study is to quantify anhydrous GGBFS and MK particles in blended cement pastes as a function of acid exposition time. This is done to evaluate their acid resistance and improve understanding of their role in the durability of cementitious material subjected to acid attack. The quantification of the anhydrous particles is measured by ^{29}Si MAS NMR, selective dissolution method and back-scattered electron (BSE) images processing while the evolution of the hydration process is evaluated using thermogravimetric analysis (TGA). This last method allows the monitoring of the mass loss occurring during the thermal decomposition of cement hydrated phases. The non-evaporable water content, or bound water, is directly function of the amount of C–S–H, portlandite, ettringite and AFm phases presented in the sample. The amounts of residual anhydrous and hydrate phases of metakaolin, slag and OPC mixtures was measured after a curing period of 28 days prior to acid immersion. The same parameters were evaluated on the altered zones of samples after 15 days, 1 and 2 months of immersion in an acetic acid solution.

2. Materials and methods

2.1. Materials

This study was conducted on three cement pastes made with OPC, designated in American Standard as GU (General Use, containing a maximum of 5% limestone filler), blended with 80% of GGBFS and with 20% of MK, respectively, as a partial cement replacement by mass of the cement. The control sample is made only of GU. No superplasticizer was added. The chemical composition of the binders is given in Table 1.

The immersion solution was composed of acetic acid (CH_3COOH), a weak organic acid with a dissociation constant p*K*a of 4.76 at 25 °C. The concentration of the acetic acid solution was 0.5 M and the pH 2.8. To avoid hydration of anhydrous phases during the acid immersion of pastes, the acetic acid was dissolved in a solvent other than water. Referring to the miscibility data of acetic acid, toluene ($C_6H_5CH_3$) was chosen. The aggressive solution was a mixture of acetic acid and toluene (0.01%). The solution was renewed every week throughout the duration of the experiment in order to maintain the pH of the solution at a value of 2.8.

Table 1
Chemical composition of binders.

Binders	%CaO	%SiO_2	%Fe_2O_3	%Al_2O_3	%MgO	%K_2O	%Na_2O	%TiO_2
GU	62.5	19.6	2.27	4.9	2.61	0.9	0.24	0.25
MK	0.03	51.65	0.68	44.7	0.08	0.34	0.08	0.12
GGBFS	37.31	36.77	0.85	7.77	13.91	0.43	0.31	0.36

2.2. Methods

The quantification of anhydrous phases consists to measure the quantities of OPC, GGBFS and metakaolin anhydrous particles as a function of acid exposition time in order to evaluate their chemical resistance. Acetic acid was diluted in toluene (0.01%) in order to avoid the presence of water causing the hydration of the anhydrous phases. Different methods were reported for the quantification of anhydrous particles of Portland cement or blended cements in order to evaluate the hydration degree of cementitious materials. These techniques included the selective dissolution method [14–18], ^{29}Si magic angle spinning nuclear magnetic resonance (MAS NMR) technique [19–21] and back-scattered electron (BSE) images processing techniques [22,23] while the quantification of the hydrated phase content was evaluated by thermogravimetric analysis (TGA). Some authors have combined the use of ^{29}Si MAS NMR and selective dissolution [24–26] while others have used the selective dissolution and image processing techniques [27]. In this study, anhydrous GGBFS and MK particles were quantified using the 3 methods. Results obtained by the different methods will be analyzed and compared.

2.2.1. Specimen making and treatment

Cement pastes were made at a water/cementitious material ratio of 0.27. Hardened cement pastes specimens are cylindrical, 100 mm high and 50 mm diameter. The specimens were demolded 24 h after pouring and stored in moist-curing room (23 °C, RH = 100%) for 27 days. Cement pastes were made according to ASTM C192/C192M procedure [55].

Samples were removed from the moist-curing room, wiped to remove water surface and then immersed in an acetic acid solution at a pH of 2.8 for 2 months at solid–liquid volume ration of 1/15. Some control specimens were kept in moist-curing room during the whole experiment. At the end of each immersion period (15 days, 1 and 2 months), specimens were wiped and dried at room temperature. The analyses were realized in the sound and altered zones of the specimens. The external altered zone was easily removed from the specimen due to shrinkage cracking. Samples were pulverised into powder to pass through a 200 mesh sieve of 74 μm apertures for the NMR analysis and pulverised into powder to particle size lower than 63 μm for the selective dissolution method. Polished flat sections were prepared for image analysis technique using standard procedure with SiC and diamond pastes as abrasive material.

2.2.2. NMR spectroscopy

Skibsted et al. [28] have shown that ^{29}Si MAS NMR spectroscopy is a very valuable tool for quantifying the silicate phases (C_2S and C_3S) in Portland cement. Due to the overlapping of resonance lines of these minerals, their amounts are obtained by decomposition of ^{29}Si MAS NMR spectra. According to Chao [26], ^{29}Si MAS NMR is not only a good method for characterizing the clinker (i.e. C_3S and C_2S) but can also be used to evaluate the amount of blast furnace slag which are essentially constituted by SiO_2, Al_2O_3 and CaO. In fact, the ^{29}Si MAS NMR spectra of hydrated cement paste consist of two parts: One related to residual anhydrous silica C_3S and C_2S (Q_0 and Q_4) and the other related to the hydrates of the chains component of C–S–H (Q_1 and Q_2). The spectrum of alite is characterized by a large broadened line ranging between −69 ppm and −74.5 ppm [26]. It consists on a monoclinic form of alite with isolated SiO_4, tetrahedra (Q_0) [29]. The spectrum of belite is illustrated

by a single narrow resonance at −71.3 ppm forming the Q_0 sites [29–31]. The ^{29}Si MAS NMR spectrum of slag is characterized by a large massive Q_0 at −74.5 ppm [32], −75 ppm [26] and −75.8 ppm [33]. The ^{29}Si MAS NMR spectrum of metakaolin indicates a large massive Q_4 ranging between −99 ppm and −105 ppm [34].

For the NMR technique, only ^{29}Si MAS NMR spectra were followed. According to the technique, only the evolution of siliceous phases can be quantified. Cross-polarization sequence was not used. However, the interaction between the nucleus such as dipolar coupling and chemical shifts anisotropy causes the line broadening and loss of accuracy of NMR spectra. To improve the spectral resolution, a sequence of magic angle spinning (MAS) has been constantly used.

The ^{29}Si MAS NMR studies were performed on a Bruker Biospin Ltd. (Milton, ON, Canada) Avance spectrometer (7.4 T) using a 4 mm CP/MAS. The ^{29}Si MAS NMR spectra were obtained using typical spinning speed of 12–15 kHz, with a rotor synchronized Hahn-Echo sequence, and relaxation delay of 30 s and 2000–10,000 scans. All NMR spectra were acquired under identical condition to allow comparison of data.

2.2.3. Selective dissolution method

Selective dissolution method, originally proposed by Luke and Glasser [14,15], was designed specifically in order to determine the reaction degree of slag. The principle of the method is to dissolve a cement paste sample in specific solvents which attack unhydrated cement components and hydration products leaving unreacted slag particles that are retained as residue at the end of the manipulation [35]. The solvents used by Demoulian et al. [36] and Luke and Glasser [14,15] consist on a solution of Ethylene Diamine Tetra acetic Acid (EDTA), a metal cation complexing agent, with triethanolamine at a pH of 11.6.

Several authors [18,24,26,36,37,17,38,39] have used the selective dissolution method to follow the hydration rate of ground granulated blast-furnace slag. In this study, the selective dissolution method was used to quantify ground granulated blast-furnace slag and metakaolin anhydrous particles in blended cement pastes as a function of acid immersion time in order to evaluate their chemical resistance.

The selective dissolution method is based on preferential dissolution. This technique preferentially dissolves the anhydrous cement particles and the hydration products leaving only the anhydrous GGBFS particles. This technique was run in triplicates on well homogenized sample of 0.25 g of blended pastes ground to <63 μm. An accurately weighed solid sample was added to a stock solution composed of:

(a) 125 ml of a solution composed of 0.05 mol/l EDTA (ethylenediaminetetraacetic acid) in 0.1 mol/l of Na_2CO_3;
(b) 12.5 ml of a 1:1 triethanolamine:water mixture;
(c) 125 ml of distilled water.

The pH of the final solution was adjusted to 11.6 with 0.1 mol/l NaOH and shaken for 30 min. The residue was filtered and dried at 105 °C for 20 h. The residue was then washed 7 times with 20 ml of distilled water and 3 times with 20 ml methanol. Residue was dried at 105 °C until constant weight.

In this study, the percentage of residual anhydrous particles present in the blended cement pastes composed of 20% MK or 80% GGBFS were determined according to the following formula [14,15]. Here, the term supplementary cement material (SCM) is used to represent GGBFS or MK:

– The degree of reaction of SCM is calculated according to the equation:

$$\alpha_{SCM}(t) = 100 - \frac{[\omega_2 + (\%SCM_{(t=0)}\%SCM_{dissolved}\omega_1) - (\%CEMENT_{(t=0)}C_r\omega_1)]}{[\%SCM_{(t=0)}\omega_1]} \quad (1)$$

where ω_1 is the weight of sample (ignited weight); ω_2 the weight of residue (105 °C dry weight); C_r the percentage of residue from cement divided by 100; $\%SCM_{(t=0)}$ the percentage of initial SCM in the blended cement; $\%CEMENT_{(t=0)}$ the percentage of initial cement in blended cement; and $\%SCM_{dissolved}$ is the percentage of SCM dissolved.

2.2.4. Image analysis method

Image segmentation is a process of image analysis that allows extracting parameters in order to establish a compact and representative description of the image content for classification or interpretation [40–43]. For the last 10 years, various image analysis methods have been developed and used to characterize some features of cement based materials [44,45], especially to study the degree of hydration of concrete [22,23,46–48].

The Backscattered electron (BSE) imaging has been widely used as a technique to examine the microstructure of cement based materials. The segmentation of backscattered electron (BSE) images has often been used to quantify the microstructure of cement pastes, including the determination of the pore structure [44], the anhydrous cement content [47,49], the aggregate particles content [50], the importance of cracks [51], the distribution of the interfacial porosity around aggregate particles [52] and the characterization of the structure of fresh cement paste [53]. Some authors have combined the use of selective dissolution and BSE image analysis techniques for quantification of the fly ash in blended cement [27] or of the slag in supersulfated cements [48].

The quality of segmentation has a direct impact on results obtained [22]. Thus, the quality of brightness and contrast of images are very important factors. Quantification of features via image analysis requires, firstly, good specimen preparation and imaging technique to produce representative images, and secondly, a feature-segmentation algorithm that is objective, precise and reproducible [54].

In this work, flat polished sections of cement pastes were observed under scanning electron microscope (SEM) in backscattered electron imaging (BSEI) mode at 500× magnification. Image segmentation was applied in order to evaluate the area fraction of the residual OPC and GGBFS anhydrous particles as a function of the acid immersion time. An algorithm is used for separating out the different phases present in the cement pastes. Images are segmented by greyscale thresholding to produce binary images of regions of interest. The grey level histogram is composed of separate peaks corresponding to distinct phases. The area of the histogram is proportional to the relative fractions of each phase.

Polished sections of blended paste samples were observed under a JEOL JSM-840A Scanning electron microscope equipped with an energy dispersive X-ray analysis system (EDXA) at 15 kV.

Interaction of an accelerated electron beam with a specimen produces a variety of elastic and inelastic collisions between electrons and atoms within the sample. Backscattered electrons (BSE) consist of high-energy electrons originating in the electron beam that are back-scattered out of the specimen interaction volume by elastic interactions with specimen atoms. Since heavy elements (high atomic number) backscatter electrons more strongly than light elements (low atomic number), BSE is proportional to the mean atomic number of the phase and are used to detect contrast between phases with different chemical compositions.

Phase discrimination is based on BSE grey level distribution. In this study, ten BSE images were captured for each sample. To simplify the analysis, all images were captured with the same magni-

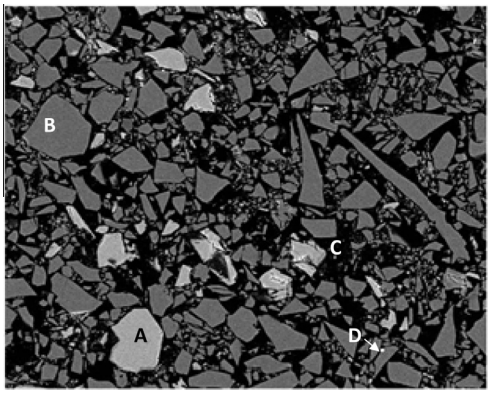

Fig. 1. BSE source image of a cement paste containing 80% GGBFS after 28 days of curing (w/binder = 0.27). Magnification = 500×. (A) GU anhydrous phase. (B) GGBFS anhydrous phases. (C) Hydrates and porosity. (D) Lead contamination due to polishing table.

fication (500×), contrast and brightness. Each image counts 1832 by 1444 pixels and 256 grey tones. Image segmentation based on thresholding method was the method used to separate the different phases. As the average BSE grey level is directly related to a phase of unique atomic number [56,57], the segmentation method used the histogram of the grey level distribution of different phases to discriminate each phase. Elemental composition measured by energy dispersive X-ray analysis (EDXA) was used to confirm the identity of each phase. Quantification is based on the number of pixel of each grey tone using an iterative algorithm.

Fig. 1 presents an example of a BSE image of a cement paste containing 80% of GGBFS after a curing period of 28 days. GU anhydrous particles appear with a lighter color than GGBFS anhydrous grains on the BSE image due to its higher atomic density. Interstitial darker color phase corresponds to hydrated phases. Black areas in the BSE image corresponds to porosity filled with resin in the polished sample preparation. Very small bright white areas correspond to lead contamination coming from the polishing table.

Fig. 2 presents the extraction of GU anhydrous phases after image segmentation with corresponding histogram.

Fig. 3 shows the GGBFS anhydrous particles extracted based on BSE grey level. This is the major phase of the material.

Fig. 4 is the result of extraction of phases with low mean atomic number. These phases correspond to the cement hydration products and porosity. The last segmentation was for the very high mean atomic number phase (Fig. 5). This corresponds to the lead contamination that is an artifact of the polishing process using soft metal (lead) table.

2.2.5. Thermogravimetric analysis (TGA)

TGA analyses were performed in alox (Al_2O_3) cups under N_2 atmosphere at a heating rate of 10 °C/min from 25 to 900 °C (TGA 7, Perkin Elmer). The non-evaporable water content (bound water) were obtained from the weight loss of samples between 105 and 900 °C corresponding to the cumulative mass of C–S–H, ettringite, portlandite and AFm phases.

3. Results

3.1. Quantification of anhydrous phases using the ^{29}Si MAS NMR spectra

In the present study, the method used consists of a preliminary characterization of anhydrous compounds (reference sample). Subsequently, the identification and quantification of phases observed in each spectrum are obtained from it fit according to reference spectra.

3.1.1. Quantification of GGBFS anhydrous grains

The calculated spectrum of the anhydrous GGBFS reference mixture containing 80% of blast furnace slag as a partial replacement by mass of cement was obtained. The chemical composition of the mixture was compared to its ^{29}Si MAS NMR spectra and the intensity of each component was adjusted according to its SiO_2 contribution in the mixture. The SiO_2 contribution of each component was obtained by dividing the number of silicon atoms of each component by the amount in the whole anhydrous mixture as presented in Table 2.

The molar C_3S/C_2S ratio was calculated using the Bogue equation in order to represent the contribution of GU in terms of C_3S and C_2S ($C_3S/C_2S = 6.43$). Then, the calculated spectrum was adjusted to the experimental spectrum in order to minimize the residue as presented in Fig. 6.

The intensities of the resonance for the subspectra of alite, belite and slag anhydrous grains were optimized to the experimental spectrum by least-squares analysis. The optimisation includes line widths, line shapes (Gaussian and/or Lorentian) and chemical shifts of peaks of each component of the anhydrous reference mixture.

The calculated spectrum consists on a region Q_0 including a fine line of C_2S at −71.3 ppm, a large broad line of C_3S at −73.94 ppm (consisting of 3 lines) and a large broad line at −75.63 ppm of GGBFS. Fig. 6 shows the decomposition of the ^{29}Si MAS NMR spec-

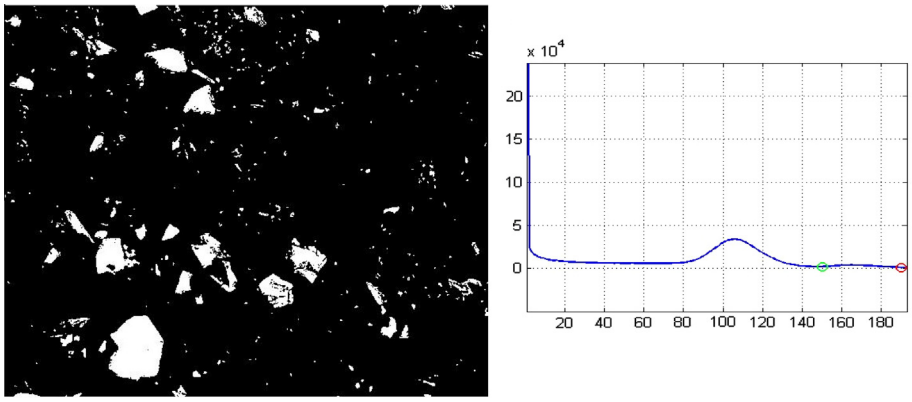

Fig. 2. Extraction of GU anhydrous particles by BSE image segmentation with corresponding histogram.

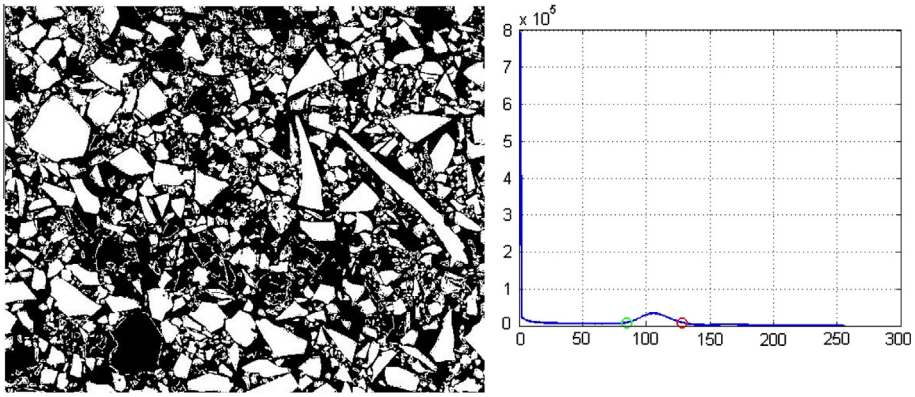

Fig. 3. Extraction of GGBFS anhydrous particles by BSE image segmentation with corresponding histogram.

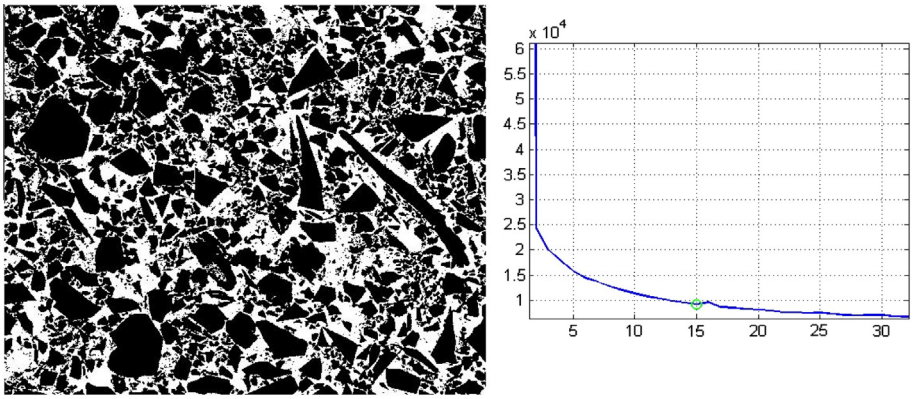

Fig. 4. BSE image of low mean atomic number phases (hydrates and porosity) extracted by image segmentation with corresponding histogram.

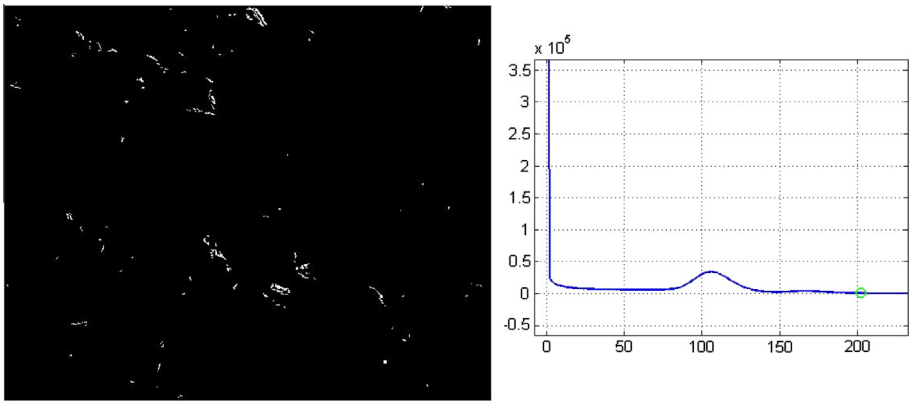

Fig. 5. Extraction of lead contamination particles (high mean atomic number phase) by BSE image segmentation with corresponding histogram.

trum of anhydrous GU blended with 80 wt% GGBFS (reference sample) including the subspectra for alite, belite, GGBFS anhydrous grain which constitutes the optimized simulation.

After the deconvolution process, the different silica bearing phases were quantified based on the fact that the intensities are proportional to the molar amount of silica provided by each phase in the anhydrous reference mixture. The intensity of the spectrum of each anhydrous phase was then multiply by its own molecular weight relative to one mole of silicon according to the stoichiometry of each phase. Values of 228.3 and 172.2 g/mole were considered for alite ($3CaO{\cdot}SiO_2$) and the belite ($2CaO{\cdot}SiO_2$), respectively.

The determination of the stoichiometry of the GGBFS ($66CaO{\cdot}61SiO_2{\cdot}7.6Al_2O_3{\cdot}34MgO$) is based on its elemental composition given a molecular weight relative to one mole of silicon of 156.26 g/mole (Table 3). The mass content of each anhydrous phase present in hydrated cement paste samples subjected to acid immersion is then calculated according to the RMN intensity considering its own molecular weight relative to one mole of silicon. As for the calculation of the anhydrous reference sample, the mass of each anhydrous phase is calculated according to the sum of the mass of all anhydrous phases in the mixture. All parameters for the adjustment of each component previously identified on the anhy-

Table 2
SiO_2 Contributions of each component of the GGBFS anhydrous mixture (reference sample).

	% in the anhydrous reference mixture (wt%)	SiO_2 (wt%)	Mass of SiO_2 (g)	Mol of SiO_2 (mole)	SiO_2 contribution (mole%)
GU	20	19.6	3.92	0.065	11.7[a]
GGBFS	80	36.77	29.42	0.489	88.3
			Reference	0.554	

[a] SiO_2 contribution of 1.6 and 10.1 (mole%) for C_2S and C_3S, respectively.

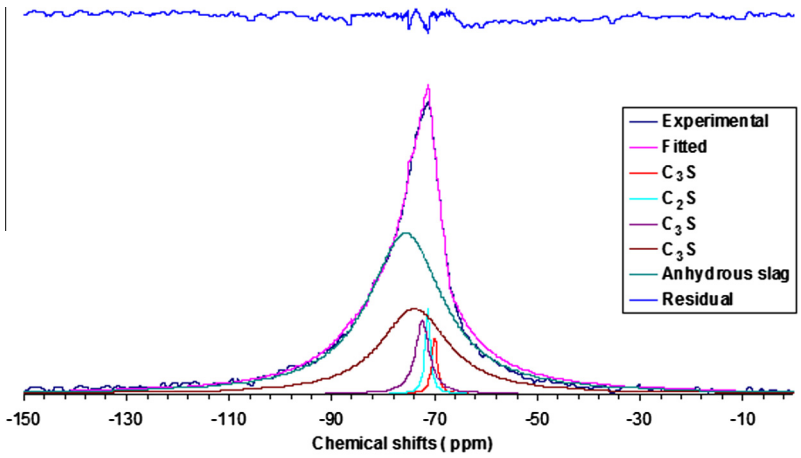

Fig. 6. ^{29}Si MAS NMR spectrum of the GGBFS anhydrous mixture (reference sample) showing the fitted, the full deconvolution and the residual subspectra.

Table 3
Mass and number of moles of each major oxide present in 100 g of GGBFS.

	GGBFS (wt%)	For 100 g of GGBFS	
		Mass (g)	Mole (mole)
CaO	37.31	37.31	0.66
SiO_2	36.77	36.77	0.61
Al_2O_3	7.77	7.77	0.076
MgO	13.91	13.91	0.34

drous reference mixture (peak position, peak width at half height) were kept constant. Results obtained for the amount of anhydrous phases in the pastes blended with GGBFS are presented in Table 4.

Fig. 7 shows a direct comparison between the resistance of GU and slag anhydrous grains as a function of the immersion time in an acetic acid solution. Over the immersion period of 2 months, amount of GU anhydrous grains drops by 48.5% while the amount of GGBFS anhydrous grains decreases by only 23.3%. ^{29}Si MAS NMR spectra showing the evolution of all anhydrous phases is shown in Fig. 8.

3.1.2. Quantification of metakaolin anhydrous grains

The quantification of metakaolin anhydrous grains was performed using the method described for GGBFS samples. The ^{29}Si MAS NMR spectrum of the metakaolin cement consists of two parts: Q_0 related to GU cement anhydrous and Q_4 related to metakaolin anhydrous grains. Q_0 peaks are formed by a thin line of C_2S at −71.3 ppm and a broad line of C_3S (consisting on 3 lines) at −73.94 ppm. Q_4 includes a wide broad line at −105.3 ppm for metakaolin anhydrous grains. Fig. 9 shows the decomposition of the ^{29}Si MAS NMR spectrum of anhydrous GU blended with 20 wt% metakaolin (reference sample). Results obtained for the amount of anhydrous phases in pastes blended with MK are presented in Table 5.

Fig. 10 presents a comparison between the resistance of GU and metakaolin anhydrous grains as a function of the immersion time in an acetic acid solution. Over the immersion period of 2 months, amount of GU anhydrous grains drops by 45.2% while the amount of MK anhydrous grains decreases by only 14.5%. The percentage of GU anhydrous phases in slag samples presents a decrease of 48.5% compared to 45.2% for MK samples. This difference may be due to the experimental precision of NMR analyzes or the fact that MK blended pastes are more chemically or mechanically resistant to acid aggression. ^{29}Si MAS NMR spectra showing the evolution of all anhydrous phases is shown in Fig. 11. It is clear from this figure that a large proportion of metakaolin is hydrated after 28 days of moist cure (initial curve) and that the acid immersion has little influence on this material. However, GU anhydrous grains are less stable in acidic solution and their content decreases rapidly with immersion time.

3.2. Quantification of anhydrous phases measured by selective dissolution method

3.2.1. Metakaolin anhydrous phases

In order to verify the application of the selective dissolution method for the cement pastes containing metakaolin, a preliminary test was conducted on samples hydrated for 28 days prior to acid immersion.

The residue obtained after the dissolution was analyzed by X-ray diffraction (Siemens D5000 X-ray diffractometer using Cu Kα radiation generated at 30 mA and 40 kV. Specimens were step-scanned as random powder mounts from 8° to 66° 2θ at 0.02°2θ steps integrated at 1.2 s $step^{-1}$) (Fig. 12). The results show the persistence of hydrated phases (C–S–H and/or C–A–S–H) represented by a large halo centered in the central part of the graph on the reticular distance of about 3.0 Å. Moreover, no trace of illite, the clay mineral present in metakaolin, appears in the residue. This would mean that metakaolin has completely reacted after a curing

Table 4
Mass content of each residual anhydrous phase evaluated as a function of the acid immersion time.

	GU		GGBFS	
	C_3S	C_2S		
Anhydrous reference mixture				
Molar mass per mole of Si	228.315	172.238	156.26	
^{29}Si NMR intensity	1.23E+09	2.53E+08	8.31E+09	
Mass as function of the ^{29}Si NMR intensity (g)	2.81E+11	4.63E+10	1.30E+12	1.62E+12
Mass content relative to ^{29}Si NMR intensity	17.31%	2.69%	80%	100%
	20%			
After 28 days of curing (before acid immersion)				
Mass as function of the ^{29}Si NMR intensity (g)	1.08E+11	2.12E+10	7.29E+11	
Mass content relative to ^{29}Si NMR intensity	6.67%	1.31%	44.94%	
	7.98%			
15 days of immersion				
Mass as function of the ^{29}Si NMR intensity (g)	9.98E+10	1.81E+10	7.01E+11	
Mass content relative to ^{29}Si NMR intensity	6.15%	1.11%	43.22%	
	7.26%			
1 month of immersion				
Mass as function of the ^{29}Si NMR intensity (g)	9.48E+10	1.12E+10	6.56E+11	
Mass content relative to ^{29}Si NMR intensity	5.84%	0.69%	40.45%	
	6.53%			
2 months of immersion				
Mass as function of the ^{29}Si NMR intensity (g)	5.98E+10	6.79E+09	5.59E+11	
Mass content relative to ^{29}Si NMR intensity	3.69%	0.42%	34.47%	
	4.11%			

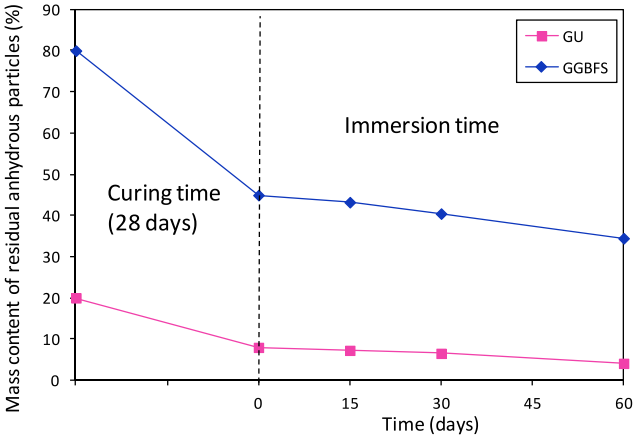

Fig. 7. Mass content of residual GU and GGBFS anhydrous grains during the acetic acid immersion of paste samples.

period of 28 days. These results show that the selective dissolution method tested is not relevant for the quantification of anhydrous metakaolin particles.

3.2.2. GGBFS anhydrous phases

Fig. 13 presents the evolution of anhydrous GGBFS particles content as a function of the acid immersion time measured by the selective dissolution method. After 28 days of moist curing (before acid immersion), 42% of slag particles were hydrated. The amount of GGBFS anhydrous particles slowly drops during acid immersion with a reduction of 22% after 2 months of immersion in a solution of acetic acid maintains at a pH of 2.8.

This result confirms the very good acid resistance of GGBFS anhydrous particles against acid attack. Data presented in Fig. 13 are mean of three sub-samples. The coefficient of variation is about 6% within triplicates.

3.3. Quantification of anhydrous phases by BSE image analysis process

3.3.1. GGBFS anhydrous phases

Fig. 14 presents a BSE image of a cement paste blended with 80% GGBFS after 28 days of hydration followed of 15 days of acid immersion (pH 2.8).

As mentioned before, GU anhydrous particles appear with a lighter color than GGBFS anhydrous grains on the BSE image due to its higher atomic density. GGBFS anhydrous particles present homogenous surfaces without any alteration. Chemical composition measured by EDXA shows that GGBFS particles are composed mainly of oxides of silicon, calcium, magnesium and aluminum. GU anhydrous particles are more affected by the acidic environment and present some alteration. GU anhydrous phases are mainly composed of oxides of calcium and silicon.

The evolution of anhydrous GU and GGBFS particles content is presented in Fig. 15 as a function of the acid immersion period. After 28 days of curing (before acid immersion) the hydration rate measured by image analysis are 56.5% and 36% for GU and GGBFS, respectively (water/binder ratio of 0.27).

After 2 months of acid immersion, the amount of anhydrous particles drops by 44% for GU and by 18% for GGBFS.

3.3.2. Metakaolin anhydrous phases

Fig. 16 presents a BSE image of a cement paste blended with 20% of metakaolin after 28 days of hydration. EDX analysis presented in Fig. 5 corresponds to anhydrous metakaolin particles. The metakaolin studied has a mean particle size of 3 μm and due to its sheet-shape; crystals are often far less than 1 μm wide. After hydration, the size of anhydrous particles decreases and becomes difficult to differentiate on the BSE images.

The BSE image presents a multitude of small areas that are very difficult to extract. The segmentation process requires the integration of other types of information based on the texture and the morphology of the metakaolin anhydrous particles. One of the main limitations of the BSE image analysis technique is spatial resolution as suggested by Scrivener [23] and results obtained with metakaolin blended pastes.

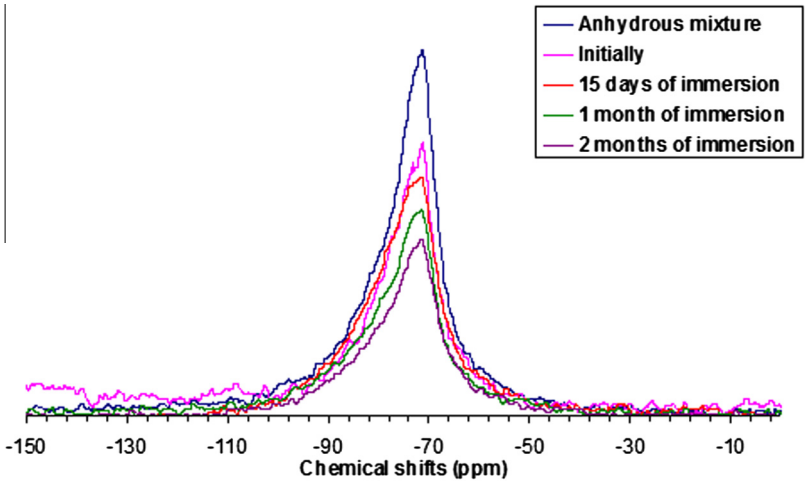

Fig. 8. ^{29}Si MAS NMR spectra of the evolution of siliceous anhydrous phases of GU and GGBFS pastes after 28 days of hydration (initial data) and during the acetic acid immersion.

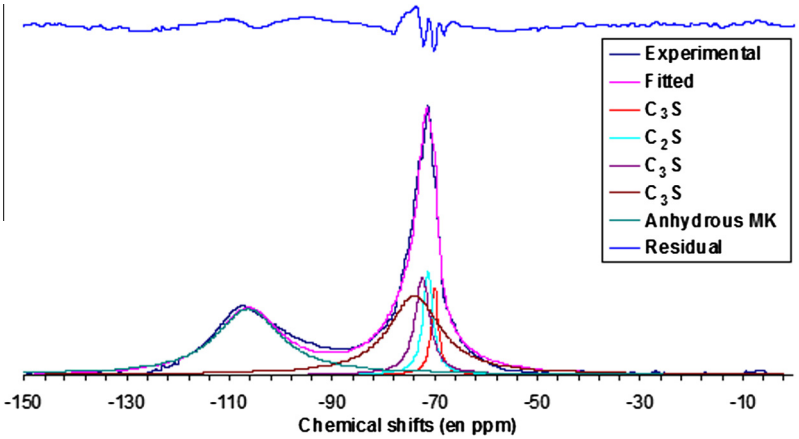

Fig. 9. ^{29}Si MAS NMR spectrum of the MK anhydrous mixture (reference sample) showing the fitted, the full deconvolution and the residual subspectra.

Table 5
Mass content of each residual anhydrous phase evaluated as a function of the acidic immersion time (metakaolin mixture).

	Clinker		MK	
	C_3S	C_2S		
Anhydrous reference mixture				
Molar mass per mole of Si	228.315	172.238	106.96	
^{29}Si NMR intensity	3.88E+09	7.98E+08	2.39E+09	
Mass as function of the ^{29}Si NMR intensity (g)	8.86E+11	1.37E+11	2.56E+11	1.28E+12
Mass content relative to ^{29}Si NMR intensity	69.25%	10.75%	20%	100%
	80%			
After 28 days of curing (before acid immersion)				
Mass as function of the ^{29}Si NMR intensity (g)	3.68E+11	2.65E+10	6.09E+10	
Mass content relative to ^{29}Si NMR intensity	28.72%	2.07%	4.75%	
	30.79%			
15 days of immersion				
Mass as function of the ^{29}Si NMR intensity (g)	3.38E+11	1.77E+10	5.65E+10	
Mass content relative to ^{29}Si NMR intensity	26.40%	1.38%	4.41%	
	27.78%			
1 month of immersion				
Mass as function of the ^{29}Si NMR intensity (g)	2.85E+11	1.63E+10	5.48E+10	
Mass content relative to ^{29}Si NMR intensity	22.30%	1.27%	4.28%	
	23.57%			
2 months of immersion				
Mass as function of the ^{29}Si NMR intensity (g)	2.12E+11	3.74E+09	5.20E+10	
Mass content relative to ^{29}Si NMR intensity	16.59%	0.29%	4.06%	
	16.88%			

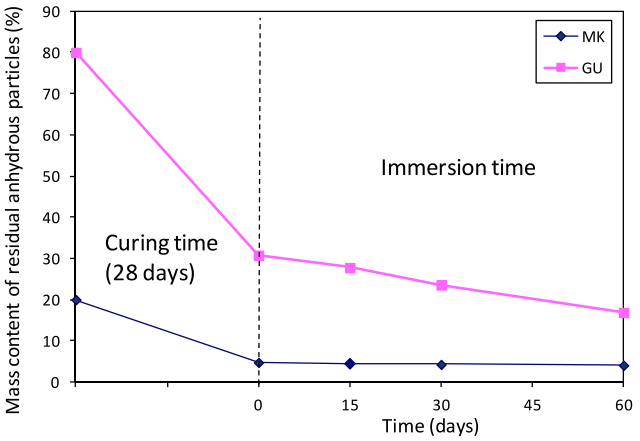

Fig. 10. Mass content of residual GU and metakaolin anhydrous grains during the acetic acid immersion of pastes.

3.4. Quantification of hydrates based on bound water content measured by TGA

The evolution of the bound water content related to hydrated phases of GU, GGBFS and MK cement pastes is shown in Fig. 17. The evolution of the bound water content related to C–S–H, portlandite, ettringite and AFm phases gives an estimate of the degree of progress of hydration. After 28 days of hydration, just before the acid immersion (time 0), the bound water content measured on GU (control), GGBFS and MK paste samples were 9.2%, 8.8% and 11.9%, respectively. These values compare well with that evaluated by subtracting the amount of residual anhydrous grains evaluated on ^{29}Si MAS NMR spectrum (Tables 4 and 5 – wt% of hydrates – 61%, 44% and 76% for GU, GGBFS and MK samples, respectively). This confirms well established facts that GGBFS shows a latent hydration while MK presents a greater rate of hydration product formation than GU cement.

The evolution of the bound water content of cement pastes after immersion in acid solution can be described as follows:

For all cement pastes, results show an increase of the bound water content at the beginning of the immersion followed by a decrease that continues to the end of the experiment. During acid immersion, the evolution of the bound water is attributed to the rate between the production and the dissolution of hydrated phases. More precisely, after 15 days of immersion, the bound water content increases reaching a maximum of 14.7% for MK blended pastes. During that period, production of hydrates is more important than dissolution. The progression of the hydration process may be due to the water trapped into the porosity of the paste samples during the moist curing. After 1 month of immersion, the

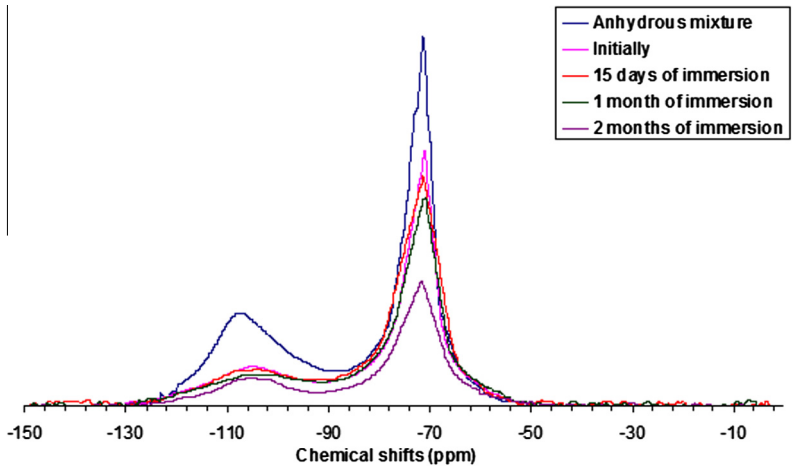

Fig. 11. ^{29}Si MAS NMR spectra for the evolution of siliceous anhydrous phases of GU and MK pastes after 28 days of hydration (initial data) and throughout the acid immersion.

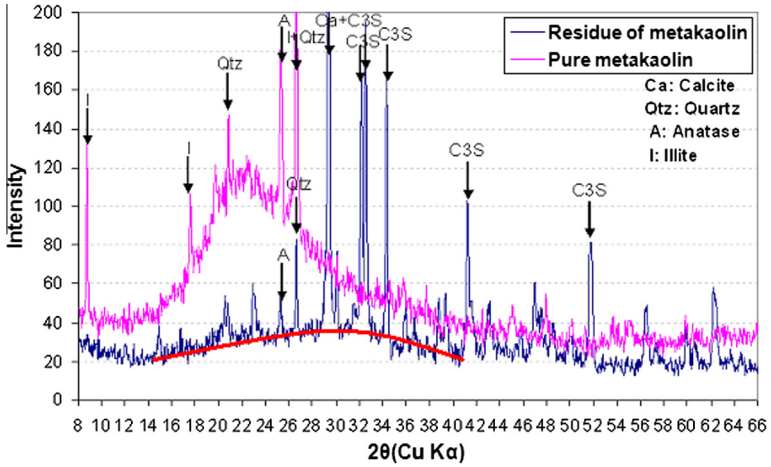

Fig. 12. XRD trace of the residue recovered from the selective dissolution method carried on a 28 days hydrated metakaolin cement paste sample.

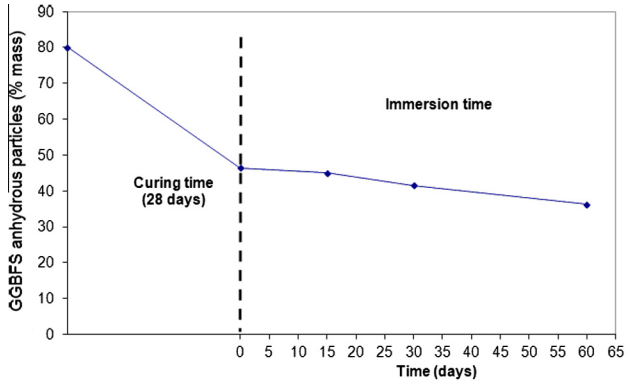

Fig. 13. Evolution of the anhydrous GGBFS particles content as a function of acid immersion time measured by selective dissolution method.

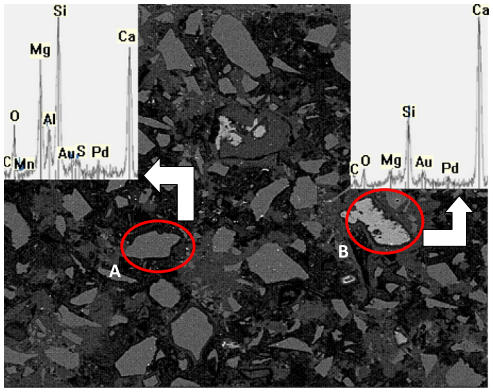

Fig. 14. BSE image of a cement paste containing 80% GGBFS after 28 days of curing (w/binder = 0.27) and 15 days of acid immersion (acetic acid, pH = 2.8). Magnification = 500×. (A) GGBFS anhydrous particle with corresponding elemental composition measured by EDXA. (B) GU anhydrous particle.

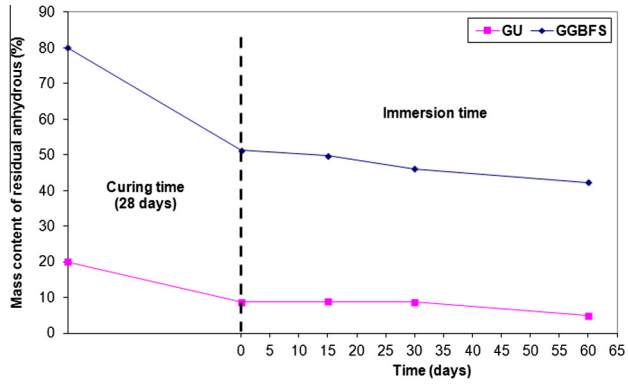

Fig. 15. Evolution of the anhydrous particles content (GU and GGBFS) as a function of acid immersion time measured by image segmentation method.

bound water content of MK paste samples begins to drop while it continues to increase for GU (control) and GGBFS paste samples and reaches their maximum content to values of 11.1% and 12.2%, respectively. It is possible that this phenomenon may be due to the greater amount of water trapped in the GGBFS and GU control pastes because of the greater porosity of these samples [58]. This may also be due to the formation of a hydrated gel as reaction product resulting from acid attack [32]. Finally, after

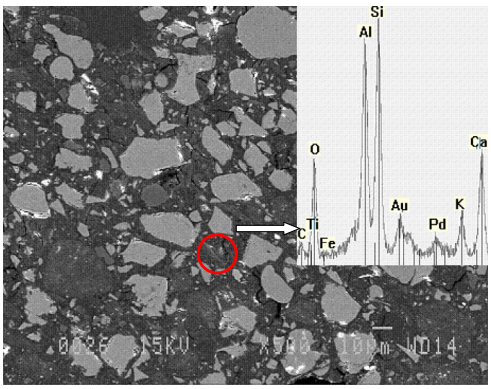

Fig. 16. BSE image of a cement paste containing 20% of metakaolin after 28 days of curing (w/binder = 0.27). Magnification = 500×.

2 months of immersion, the bound water content of all samples decreases to values of 10.4%, 11.2% and 13.5% for GU, GGBFS and MK samples, respectively. It is not clear what is the real effect of the hydrated gel formation on the bound water content but these results show that the degree of hydration is an important parameter involved in the stability of hydrated pastes in an acidic environment. In a general way, higher hydration rate, as shown by MK samples, improves the microstructure of cement pastes contributing to improve the transfer properties of the material. Nevertheless, in this study, although the GU control pastes show a higher hydration level than the GGBFS pastes, the latter present a smaller drop in the quantity of both hydrated phases and anhydrous grains after acid immersion. These results support the fact that the chemical composition of both the hydrates formed and anhydrous phases is very important for the good behavior of cement pastes subjected to an acid medium [6–9].

4. Discussion

4.1. Comparison between selective dissolution and BSE image analysis techniques

The selective dissolution technique used here is only applicable for the quantification of ground granulated blast-furnace slag anhydrous particles. This method is not applicable, in the present form, to other supplementary cementing material as metakaolin because residues other than anhydrous metakaolin particles were found after chemical dissolution. In the same way, the BSE image analysis technique was not appropriate for metakaolin blended pastes because metakaolin particle grain size is too fine to be conveniently detected on the BSE images. Spatial resolution is known as one of the main issues of BSE imaging technique [23].

The amount of GGBFS anhydrous particles measured by both methods, selective dissolution and images analysis, was of the same order of magnitude. But in a general way, the BSE image analysis method tends to overestimate the amount of anhydrous particles. Scrivener et al. [47] found that for a cement paste analysis of ten fields at 400× was sufficient to give a standard error of around 0.6%. In the same way, Mouret et al. [22] showed that a magnification of 200× is sufficient to give an error of <0.2% for measurement of 30 images to determine anhydrous phases in pastes and mortars. In this study, 10 images taken at 500× magnification were integrated to quantify GGBFS and GU anhydrous particles. Results obtained were in the same order of magnitude of those measured by selective dissolution method.

In the selective dissolution method, clinker phases are not completely dissolved. Only ettringite and ferrite phases were

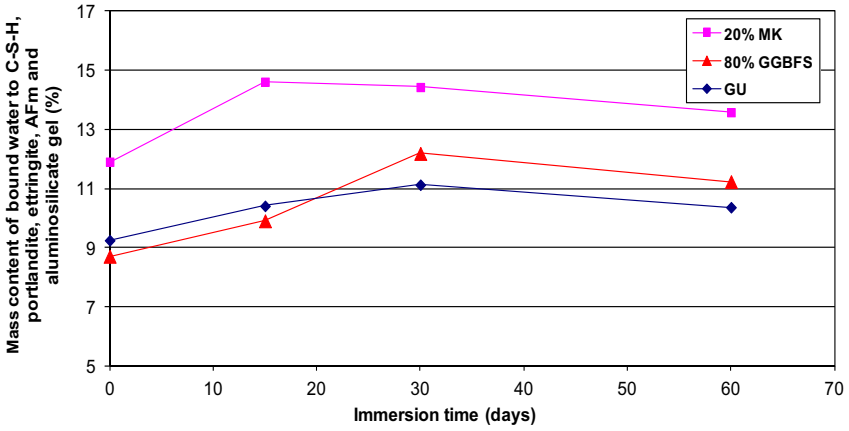

Fig. 17. Evolution of the bound water content related to hydrated phases (C–S–H, portlandite, ettringite and AFm) and aluminosilicates gel formed during the acetic acid immersion of blended paste samples.

Table 6
Comparison of the content of anhydrous particles measured by ^{29}Si MAS NMR, image analysis (BSEI) and selective dissolution (SD).

	Degree of hydration (%) after 28 days of moist curing			Drop in the anhydrous particle content (%) after 2 months of acid immersion		
	RMN	BSEI	SD	RMN	BSEI	SD
GU	60.2	56.6		48.6	43.8	
GGBFS	43.8	36.0	42.0	23.3	17.5	21.9
MK	76.2			14.5		

completely dissolved in hydrated cement pastes and hydrotalcite was observed in the residues by XRD [39]. But, in a general way, both methods are well adapted for estimation of the anhydrous particles content of blended pastes containing GGBFS.

4.2. Comparison with results obtained by ^{29}Si MAS NMR

The quantification of the residual anhydrous particles was also carried out by ^{29}Si MAS NMR. For that technique, the anhydrous phases were quantified after conducting several iterations in order to have the minimum of residue between the experimental and the calculated spectrum. The iterations performed reflect the evolution of the mass fraction of each siliceous anhydrous phase in the mixture. Table 6 presents the hydration degree of each component of blended cement after the moist cure of 28 days for the 3 techniques used and the drop in the anhydrous particles content measured after 2 months of acid immersion. Data measured by image are under those measured by NMR. The anhydrous particle content seems overestimate by the image analysis technique. One of the difficulties of this technique is the definition of clear boundaries between phases. It is possible here that hydrated GGBFS or GU particles (inner products at the surface of anhydrous particles) were not well defined. On the other hand, the advantage of the ^{29}Si MAS NMR techniques is that it is applicable to any material containing silica regardless of particle size and chemical and mineralogy composition of its constituents. The largest disadvantage of the technique is its sophistication and the long spectrum acquisition time which is nearly 24 h.

4.3. Resistance of GU, GGBFS and MK anhydrous particles subjected to acid acetic immersion

Results presented in Table 6 show that among the binders tested, GU anhydrous particles are the most attacked in an acid solution with a considerable drop reaching 48.6% after 2 months of immersion compared to the slight decrease of 23.3% measured for GGBFS anhydrous particles. Metakaolin anhydrous particles are the most resistant against the acetic acid attack with a drop of only 14.5%. This implies that the porosity will increase dramatically with acid exposure time for binders principally made of GU cement due to the high dissolution rate of anhydrous grains. These data are consistent with measurements of mass loss and degraded depth measured on blended pastes and mortars [6–9,58]. The chemical resistance of anhydrous particles as well as hydrated phases are important parameters to the durability of cementitious materials against acid attack. The dissolution of phases leads to porosity increased, which is directly related to increased degradation kinetics. For durability of concrete in acidic medium, it is important that the concrete is as impermeable as possible but also that these constituents can chemically be resistant to acids. The ground granulated blast furnace slag and metakaolin allow good chemical resistance against organic acids represented here by acetic acid and will retain their integrity for a longer period of time. This means that chemically resistant particles will be less dissolved and thus will prevent the increasing porosity of the matrix. The best binders to limit the acid attack are those which are impermeable (physical properties) and acid resistant (chemical properties).

5. Conclusion

This study reports the results of an experimental investigation on the quantification of anhydrous particles and hydrated phases content in blended cement pastes as a function of acid exposition time in order to evaluate their chemical resistance. Cement pastes made with OPC, GGBFS and MK were moist cured for 28 days and then immersed in an acetic acid solution at a pH of 2.8 for a period of 2 months. The quantification of the anhydrous phases was carried out using ^{29}Si MAS NMR, selective dissolution and image processing techniques.

^{29}Si MAS NMR spectra allows to quantify the siliceous anhydrous phases in the blended cement pastes as the area under the peak corresponds to the number of moles of silicon atoms present in the given phase. The advantage of the ^{29}Si MAS NMR techniques is that it is applicable to any material containing silica regardless of particle size and chemical and mineralogy composition of its constituents.

The selective dissolution technique used is only applicable for the quantification of GGBFS anhydrous particles. This method is not applicable to metakaolin because residues other than anhydrous metakaolin particles were found after chemical dissolution. In the same way, the BSE image analysis technique was not appropriate for metakaolin blended pastes because metakaolin particle grain size is too fine to be conveniently detected on the BSE images.

After 28 days of hydration, around 58%, 40% and 76% of OPC, GGBFS, and MK particles were hydrated. The amount of anhydrous particles drops for all materials during acid immersion with values of 46%, 22%, and 14.5% for OPC, GGBFS, and MK respectively after 2 months of acid immersion. This demonstrates the good chemical resistance of MK and GGBFS anhydrous particles against acid attack. All methods, NMR, selective dissolution and images analysis, gave results of the same order of magnitude even if the image analysis method tends to overestimate the quantity of anhydrous particles.

The degree of hydration is an important parameter involved in the stability of hydrated pastes in an acidic environment. In a general way, higher hydration rate improves the microstructure of cement pastes contributing to improve the transfer properties of the material. Nevertheless, in this study, although the OPC control pastes show a higher hydration level than the GGBFS pastes, the latter present a smaller drop in the quantity of both hydrated phases and anhydrous grains after acid immersion. GGBFS samples will retain their integrity for a longer period of time. These results support the fact that the chemical composition of both the hydrates formed during hydration process and remaining anhydrous phases is very important for the behavior of cement pastes subjected to an acid medium.

Acknowledgments

This study has been supported by the National Science and Engineering Research Council of Canada (NSERC) and by the Fonds de recherche sur la nature et les technologies of the Province of Québec (FQRNT).

References

[1] Pavlík V. Corrosion of hardened cement paste by acetic and nitric acids, part II: formation and chemical composition of the corrosion products layer. Cem Concr Res 1994;24:1495–508.
[2] Pavlík V. Effect of carbonates on the corrosion rate of cement mortars in nitric acid. Cem Concr Res 2000;30:481–9.
[3] Biczók I. Concrete corrosion, protection of concrete. Budapest: Verlag der Ungarischen Akademie der Wissenschaften; 1960. p. 10–20.
[4] Moskvin VM, Rubetskaya TV, Ljubarskaya GV. Concrete corrosion in acidic media and methods for its investigation. Beton Zhelezobeton, Moscow 1971;10:10–2.
[5] Bertron A, Escadeillas G, Duchesne J. Attack of cement pastes exposed to organic acids in manure. Cem Concr Compos 2005;27:898–909.
[6] Oueslati O, Duchesne J. The effect of SCMs and curing time on resistance of mortars subjected to organic acids. Cem Concr Res 2012;42:205–14.
[7] Oueslati O, Duchesne J. Acetic acid attack of cement matrix: evaluation of durability parameters. In: Palomo Á, Zaragoza A, Agüí J, editors. Proceeding of the 13th international congress on the chemistry of cement, Madrid, July 3–8, 2011. p. 483–4.
[8] Oueslati O, Duchesne J. Impact of acetic acid attack on the chemical, physical and mineralogical evolution of cement pastes. In: Godbout S, editor. Proceeding of the 7th international symposium on cement based materials for a sustainable agriculture (CSAS), Quebec City, Canada, September 18–21, 2011. p. 28–39.
[9] Oueslati O, Duchesne J. Acetic acid attack of blended cement pastes. In: Alexander MG, Bertron A, editors. Concrete in aggressive aqueous environments – performance, testing and modelling, Toulouse, 3-5 June, vol. 63. Rilem publication S.A.R.L, PRO; 2009. p. 108–15.
[10] Bertron A, Escadeillas G, Duchesne J. Degradation of cement pastes by organic acids. Mater Struct 2007;40:341–54.
[11] Macias A, Goñi S, Madrid J. Limitations of Köch–Steinegger test to evaluate the durability of cement pastes in acid medium. Cem Concr Res 1999;29:2005–9.
[12] Shi C, Stegemann JA. Acid corrosion resistance of different cementing materials. Cem Concr Res 2000;30:803–8.
[13] Beddoe RE, Dorner HW. Modelling acid attack on concrete: part I. The essential mechanisms. Cem Concr Res 2005;35:2333–9.
[14] Luke K, Glasser FP. Selective dissolution of hydrated blast furnace slag cements. Cem Concr Res 1987;17:273–82.
[15] Luke K, Glasser FP. Internal chemical evolution of the constitution of blended cements. Cem Concr Res 1988;18:495–502.
[16] Demoulian E, Vernet C, Hawthorn F, Gourdin P. Détermination de la teneur en laitier dans les ciments par dissolutions sélectives. In: 7th International congress on the chemistry of cement: communications, vol. 2. Editions Septima, Paris; 1980. p. III151–6.
[17] Goguel R. A new consecutive dissolution method for the analysis of slag cements. Cem Concr Aggr 1995;17:84–91.
[18] Lumley JS, Gollop RS, Moir GK, Taylor HFW. Degrees of reaction of the slag in some blends with Portland cement. Cemn Concr Res 1996;26:139–51.
[19] Zanni H, Cheyrezy M, Maret V, Philippot S, Nieto P. Investigation of hydration and pozzolanic reaction in reactive powder concrete using ^{29}Si NMR. Cem Concr Res 1996;26:93–100.
[20] Kroyer H, Lindgreen H, Jakobsen HJ, Skibsted J. Hydration of Portland cement in the presence of clay minerals studied by ^{29}Si and ^{27}Al NMR spectroscopy. Cem Concr Res 2003;15:103–12.
[21] Tong Y, Du H, Fei L. Hydration process of beta-dicalcium silicate followed by mas and cp/mas nuclear magnetic resonance. Cem Concr Res 1991;21:355–8.
[22] Mouret M, Ringot E, Bascoul A. Image analysis: a tool for the characterisation of hydration of cement in concrete-metrological aspects of magnification on measurement. Cem Concr Compos 2001;23:201–6.
[23] Scrivener KL. Backscattered electron imaging of cementitious microstructures: understanding and quantification. Cem Concr Compos 2004;26:935–45.
[24] Dyson HM, Richardson IG, Brough AR. A combined ^{29}Si MAS NMR and selective dissolution technique for the quantitative evaluation of hydrated blast furnace slag cement blends. Am Ceram Soc 2007;90:598–602.
[25] Brunet F, Charpentier T, Chao CN, Peycelon H, Nonat A. Characterization by solid-state NMR and selective dissolution techniques of anhydrous and hydrated CEM V cement pastes. Cem Concr Res 2010;40:208–19.
[26] Chao CN. Étude sur l'hydratation des ciments composés CEM V – application au comportement à long terme des bétons. Thèse de Doctorat, spécialité Chimie-Physique Université de Bourgogne; 2007. p. 216.
[27] Haha MB, De Weerdt K, Lothenbach B. Quantification of the degree of reaction of fly ash. Cem Concr Res 2010;40:1620–9.
[28] Skibsted J, Jakobsen HJ, Hall C. Quantification of calcium phases in Portland cements by ^{29}Si MAS NMR spectroscopy. J Chem Soc Faraday Trans 1995;91:4423–30.
[29] Skibsted J, Jakobsen HJ. Charaterization of the calcium silicate and aluminate phases in anhydrous and hydrated Portland cements by (27)Al and (29)Si MAS NMR spectroscopy. In: Colombet P, Grimmer AR, Zanni H, Sozzani P, editors. Nuclear magnetic resonance spectroscopy of cement-based materials. Berlin: Springer-Verlag; 1998.
[30] Grimmer AR, Zanni H. (29)Si NMR study of chemical shift tensor anisotropy of tricalcium silicate. In: Colombet P, Grimmer AR, Zanni H, Sozzani P, editors. Nuclear magnetic resonance spectroscopy of cement-based materials. Berlin: Springer-Verlag; 1998.
[31] Hansen MR, Jakobsen HJ, Skibsted J. ^{29}Si chemical shift anisotropies in calcium silicates from high-field ^{29}Si MAS NMR spectroscopy. Inorg Chem 2003;42:2368–77.
[32] Bertron A, Escadeillas G, Duchesne J. Cement pastes alteration by liquid manure organic acids: chemical and mineralogical characterization. Cem Concr Res 2004;34:1823–35.
[33] Schneider J, Cincotto MA, Panepucci H. ^{29}Si and ^{27}Al high-resolution NMR characterization of calcium silicate hydrate phases in activated blast furnace slag paste. Cem Concr Res 2001;31:993–1001.
[34] Bich C. Contribution à l'étude de l'activation thermique du kaolin: évolution de la structure cristallographique et activité pouzzolanique. Thèse de doctorat, INSA-Lyon; 2005. 264 p.
[35] Sisomphon K, Zhang MH, Zhang SQ, Qi F, Kor HK. Estimation of slag content and water-to-cementitious material ratio of hardened concrete. In: 31st Conference on our world in concrete & structures, 16–17 August 2006, Singapore.
[36] Demoulian E, Vernet C, Hawthorn F, Gourdin P. Slag content determination in cements by selective dissolution. In: Proceedings of the 7th international congress on the chemistry of cement, Paris, France; 1980. p. 151–6.
[37] Levelt VFJ, Vriezen EB, Galen RV. Determination of the slag content of BFS cements by means of a solution method. Zem Kalk Gips 1982;35(2):96–9.
[38] Escalante JI, Gomez LY, Johal KK, Mendoza G, Mancha H, Mendez J. Reactivity of blast-furnace slag in Portland cement blends hydrated under different conditions. Cem Concr Res 2001;31(10):1403–9.
[39] Kocaba V, Gallucci E, Scrivener KL. Methods for determination of degree of reaction of slag in blended cement pastes. Cem Concr Res 2012;42(3):511–25.

[40] Collette B, Donnay JP, Nadasdi I. Essai de discrimination du tissu urbain par segmentation d'image. Mappe Monde 1991;4:31–5.
[41] Zouagui T, Benoit-Cattin H, Odet C. Image segmentation functional model. Patt Recog 2004;37:1785–95.
[42] Benoit-Cattin H, Zouagui T, Odet C. Functional model and object oriented programming for image segmentation methods. In: International conference on quality control by artificial vision, QCAV, 21–23 May, Le Creusot, France; 2001. p. 391–4.
[43] Fu KS, Mui JK. A survey on image segmentation. Patt Recog 1981;13:3–15.
[44] Lange DA, Jennings HM, Shah SP. Image analysis techniques for characterization of pore structure of cement based materials. Cem Concr Res 1994;24:841–53.
[45] Elsen J, Lens N, Aarre T, Quenard D, Smolej V. Determination of the W/C ratio of hardened cement paste and concrete samples on thin sections using automated image analysis techniques. Cem Concr Res 1995;25:827–34.
[46] Mouret M, Bascoul A, Escadeillas G. Study of the degree of hydration of concrete by means of image analysis and chemically bound water. Adv Cem Bas Mater 1997;6:109–15.
[47] Scrivener KL, Patel HH, Pratt PL, Parrott LJ. Analysis of phases in cement paste using backscattered electron images, methanol adsorption and thermogravimetric analysis. In: Proceeding material research society symposium, microstructural development during the hydration of cement, vol. 85; 1987. p. 67–76.
[48] Gruskovnjak A, Lothenbach B, Winnefeld F, Munch B, Renato F, Ko SC, et al. Quantification of hydration phases in supersulfated cements: review and new approaches. Adv Cem Res 2011;23(6):265–75.
[49] Zhao H, Darwin D. Quantitative backscattered electron analysis for cement paste. Cem Concr Res 1992;22:695–706.
[50] Yang R, Buenfeld NR. Binary segmentation of aggregate in SEM image analysis of concrete. Cem Concr Res 2001;31:437–41.
[51] Darwin D, Abou-Zeid MN, Ketcham KW. Automated crack identification for cement paste. Cem Concr Res 1995;25:605–16.
[52] Head MK, Buenfeld NR. Measurement of aggregate interfacial porosity in complex, multi-phase aggregate concrete: binary mask production using backscattered electron, and energy dispersive X-ray images. Cem Concr Res 2006;36:337–45.
[53] Barrioulet M, Saada R, Ringot E. A quantitative structural study of fresh cement paste by image analysis: part 1. Image processing. Cem Concr Res 1991;21:835–43.
[54] Wong HS, Head MK, Buenfeld NR. Pore segmentation of cement based materials from backscattered electron images. Cem Concr Res 2006;36:1083–90.
[55] ASTM Standard C192/C192M. Standard practice for making and curing concrete test specimens in the laboratory. ASTM International, West Conshohocken, PA; 2007.
[56] Jones MP. Applied mineralogy: a quantitative approach. London; Norwell, MA: Graham & Trotman; 1987.
[57] Gu Y. Automated scanning electron microscope based mineral liberation analysis an introduction to JKMRC/FEI mineral liberation analyser. J Min Mater Charact Eng 2003;2:33–41.
[58] Oueslati O. Durabilité des matériaux cimentaires soumis aux acides organiques. Résistance chimique mécanique et de corrosion. Thèse de Doctorat, Université Laval, Canada; 2011. p. 370.